Preparation of MoOx (x = 2, 3) Crystallites Influenced by Hydrochloric Acid†

Hanmei Hu*, Junchan Xu, Xinqing Ge, Mei Sun, Han Xuan and Kehua Zhang

School of Materials and Chemical Engineering, Anhui Jianzhu University, Hefei, P.R. China

*Corresponding author: E-mail: hmhu@ustc.edu

In this work, one-pot hydrothermal route has been presented to synthesize 3D MoO_2 nanoplate-based microspheres and 1D MoO_3 nanobelts and nanowires. The products are characterized by X-ray diffraction, field-emission scanning electron microscopy and UV-visible absorption spectrum. The experimental results reveal that the dosage of hydrochloric acid seriously influences the phase and morphology of molybdenum oxides. The optical properties of the synthesized 3D MoO_2 nanoplate-based microspheres and 1D MoO_3 nanobelts and nanowires are studied through the UV-visible absorption spectra.

Keywords: Molybdenum oxides, Hydrothermal synthesis, Optical property.

INTRODUCTION

Molybdenum oxides MoO_x (x = 2, 3), an important semi-conductor and has been widely used in electrode materials, catalyst, gas sensing, photochromic devices[1-4] due to their multiple valence and high thermal and chemical stability. MoO_2 crystallizes mainly in three polymorphic forms[5], including monoclinic, tetragonal and hexagonal phase. Wherein the monoclinic and tetragonal phases are common forms and the hexagonal phase is the unstable phase. MoO_3 also exists in three polymorphs[6], *i.e.*, orthorhombic α-MoO_3, monoclinic β-MoO_3 and hexagonal h-MoO_3. Among them, α-MoO_3 is a thermodynamically stable phase, β-MoO_3 and hexagonal h-MoO_3 are attributed to metastable phases. Up to date, a great deal of efforts have been made to synthesize molybdenum oxides with different morphologies, including MoO_2 nano-rods[7], MoO_2 nanowire arrays[8], MoO_2 hollow microchannels[9], MoO_2 hollow core-shell microspheres[10], MoO_3 nanorods[11], MoO_3 whiskers[12], MoO_3 nanobelts[6], MoO_3 hollow micro-spheres[13], MoO_3 flower-like nanobelt arrays[14], *etc*. Herein, we demonstrate that 3D MoO_2 nanoplate-based microspheres and 1D MoO_3 nanobelts and nanowires are controllably synthe-sized through an easily operated hydrothermal method. It is worthwhile to note that MoO_x (x = 2, 3) products with special morphology can be successfully fabricated by only slightly tuning the dosage of hydrochloric acid in our designed reaction system.

EXPERIMENTAL

General procedure: In a typical procedure, 1 mmol $(NH_4)_6Mo_7O_{24}\cdot4H_2O$ (AHM), 2 mmol citric acid ($C_6H_8O_7\cdot H_2O$) and 3 mmol Na_2CO_3 were successively dissolved into 25 mL (or 15mL) distilled water in a 40 mL Teflon-lined stainless steel autoclave. After stirring for 15 min, 5 mL (or 15 mL) diluted HCl (5 %) was subsequently added into the above solution. The solution total volume was kept at 30 mL. The obtained reaction mixture was stirred for an additional 0.5 h. Then, the autoclave was sealed and maintained at 200 ºC for 12 h. After cooling down to room temperature naturally, MoO_2 (or MoO_3) precipitation was filtered out, washed with distilled water and ethanol for several times and then finally dried in a vacuum at 60 ºC for 6 h. The related comparative experiments were listed in Table-1.

Detection method: The phases of samples were analyzed by X-ray diffraction (XRD) on a Philips X'Pert PRO SUPER X-ray diffractometer. The morphologies of the obtained products were recorded on a Field-emission scanning electron micro-scope (FESEM, JSM-6700F). The optical properties of the samples were investigated by using a UV-visible spectrophoto-meter (UV-5500PC).

RESULTS AND DISCUSSION

X-Ray diffraction technique was used to demonstrate the phase and crystal structure of as-prepared molybdenum oxides

TABLE-1
EXPERIMENTAL CONDITION OF SAMPLES AT 200 °C, TIME 12 h

No.	$(NH_4)_6Mo_7O_{24}\cdot4H_2O$ (mmol)	Citric acid (mmol)	Na_2CO_3 (mmol)	5 % HCl (mL)	H_2O (mL)	Phase of products
1	1	2	3	5	25	Monoclinic MoO_2
2	1	2	3	15	15	MoO_3 (main phase: orthorhombic)
3	1	2	3	0	30	Hexagonal MoO_2 and monoclinic MoO_3
4	1	2	3	10	20	OrthorhomicMoO_3 and monoclinic MoO_2
5	1	2	3	25	5	Monoclinic MoO_2 and orthorhombic MoO_3

products, as shown in Fig. 1. Fig. 1(a) is the XRD pattern of the products prepared with the dosage of 5 mL HCl (5 %). All the diffraction peaks can be indexed as monoclinic MoO_2, in good agreement with the reported data (JCPDS No. 32-0671). Fig. 1(b) is the XRD pattern of the products obtained with the adding amount of 15 mL HCl (5 %). Most of the reflection peaks can be indexed to the orthorhombic phase of α-MoO_3 (JCPDS No. 35-0609). Three peaks with lower intensity (Marked by "#" in Fig. 1(b)) can be attributed to hexagonal h-MoO_3 (JCPDS No. 21-0569), which is one type of metastable phase of MoO_3.
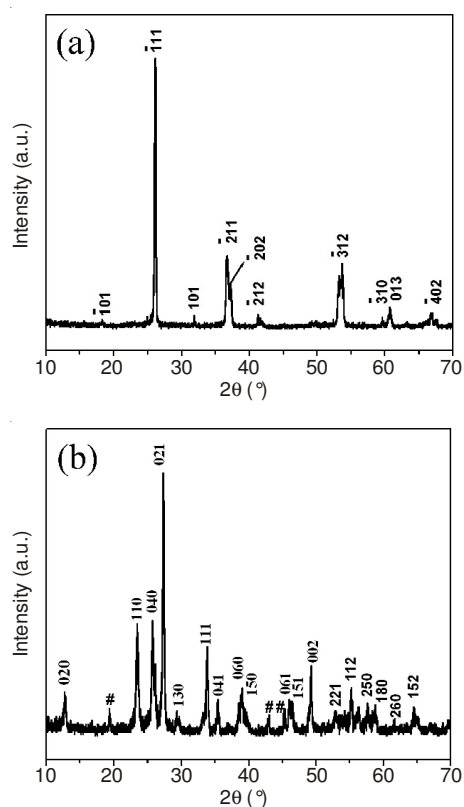

Fig. 2.   (a,b) FESEM images of MoO_2 products, (c,d) FESEM images of MoO_3 products

lengths are in the range of 10-20 μm. The diameters and the lengths of MoO_3 nanowires are estimated to be 30-40 and 15-25 μm, respectively.

In the present designed synthetic system, the usage and amount of hydrochloric acid play important roles in controlling the phase and morphology of molybdenum oxides. To reveal the leverage of hydrochloric acid, a series of comparative experiments were carried out by only changing the dosage of hydrochloric acid while keeping other conditions unchanged. The experimental results were shown in Fig. 3. If HCl was not used, only little products (Sample 3) were obtained [Fig. 3(a) and (b)]. From the XRD pattern of Fig. 3(a), it may deduce that the main phase was unstable hexagonal phase of MoO_2 (JCPDS No. 50-0739), which was scarcely reported in the literature. In addition, a small quantity of monoclinic β-MoO_3 (JCPDS No. 80-0347) was also detected [marked by "*" in Fig. 3(a)], which was another type of metastable phase of MoO_3. The morphologies of products were submicrospheres with diameters of 500-1000 nm and some spheres tended to aggregate together to form multiple microspheres [Fig. 3(b)].

When 10 mL HCl was added into the reaction solution, the obtained products (sample 4) were the mixture in of major hexagonal MoO_3 and minor monoclinic MoO_2 (marked by "*" in Fig. 3(c)). According to the corresponding morphology displayed in Fig. 3(d), MoO_3 nanobelt-based bundles as well as some MoO_2 microspheres were observed and these nano-belts tended to aggregate together to form sheet-like micro-structure. if the dosage of HCl was increased to 25 mL, the synthesized products (sample 5) were the mixture of major monoclinic MoO_2 and minor hexagonal MoO_3 (marked by "*" in Fig. 3(e)). From the correlative picture of Fig. 3(f), bigger

Fig. 1.   XRD patterns of (a) MoO_2 microspheres and (b) MoO_3 nanobelts and nanowires

Fig. 2(a) and (b) present the FESEM images of MoO_2 products (sample 1), which indicate that the products are composed of irregular sphere-like microcrystals with the sizes of 1.3-3.5 μm. From the enlarged image of an individual microsphere [the inset of Fig. 2(a)], we can see the building blocks are nanoplates with the thicknesses of 60-90 nm. Fig. 2(c) and (d) show the morphology of MoO_3 products (sample 2), which indicate that belt-like (70 %) and wire-like (30 %) are found in the products. The widths and thicknesses of MoO_3 nanobelts are 100-200 and 30-50 nm, respectively and the
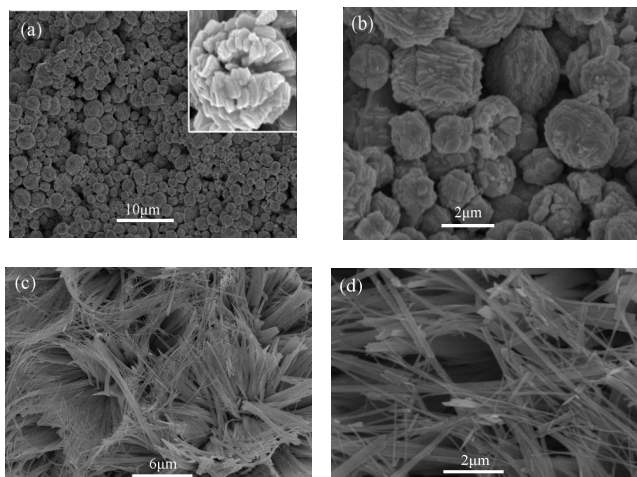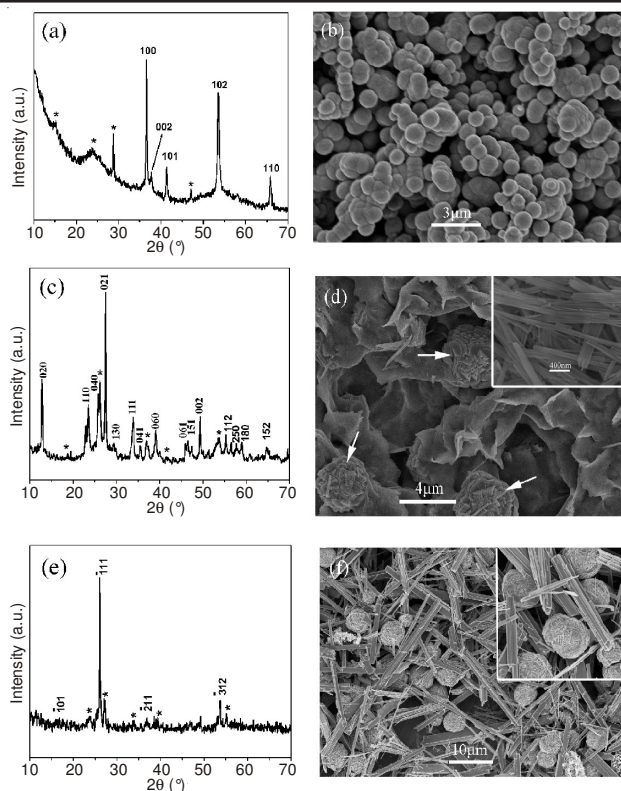
Fig. 3. XRD patterns and FESEM images of the products prepared at different conditions: (a,b) 0 mL 5 % HCl; (c,d) 10 mL 5 % HCl; (e,f) 25 mL 5 % HCl

Fig. 4. UV-visible absorption spectrum and band gap energy (inset) of (a) MoO$_2$ microspheres and (b) MoO$_3$ nanobelts and nanowires

MoO$_2$ microspheres and longer MoO$_3$ belt-based bundles were easily distinguished.

Based on the comparative experimental analysis, a conclusion could be drawn that the dosage of HCl really influenced the phase and morphology of MoO$_x$. At lower acidity (5 mL 5 % HCl), Mo(VI) were completely reduced to Mo(IV) by citric acid and pure monoclinic MoO$_2$ nanoplate-based microspheres could be obtained (sample 1). At moderate acidity (15 mL 5 % HCl), the reduction reaction were effectively restrained and MoO$_3$ nanobelts and nanowires were produced (sample 2). However, at higher acidity (25 mL 5 % HCl), Mo(VI) were partially reduced to Mo(IV) by excessive reducing acid HCl (sample 5). So, the desired molybdenum oxides products could be successfully achieved by adjusting the appropriate dosage of HCl in this system.

Fig. 4(a) and (b) exhibit the UV-visible absorption spectrum as well as band gap energy (inset) for MoO$_2$ microspheres and and MoO$_3$ nanobelts and nanowires. The optical band gap E$_g$ can be determined by the Tauc's equation of $(\alpha h\nu)^n = B(h\nu - E_g)$ for a semiconductor, where B is the edge-width parameter, hν is the photon energy and the value of n is 2 for allowed direct transition of MoO$_x$. The plot of $(\alpha h\nu)^2$ *versus* hν is shown in the inset of Fig. 4. By extrapolating the straight line to $(\alpha h\nu)^2 = 0$, the band gap E$_g$ of MoO$_2$ microspheres is calculated to be 3.92 eV and that of MoO$_3$ nanobelts and nanowires is estimated to be 3.06 eV.

Conclusion

A simple and effective route is presented to controllably prepare nanoplate-based 3D MoO$_2$ microspheres and 1D MoO$_3$ nanobelts an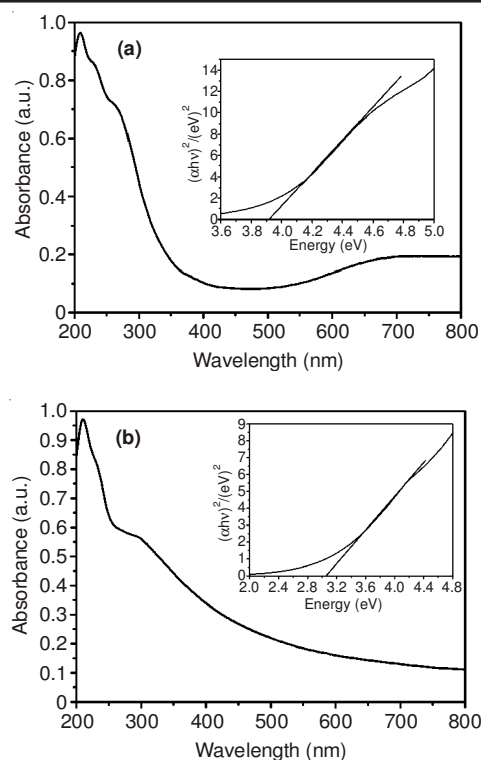d nanowires. In the present designed reaction system, the introduction and amount of hydrochloric acid is found play important roles in controlling the phase and morphology of molybdenum oxides. According to the UV-visible absorption spectrum, the band gap E$_g$ of MoO$_2$ microspheres is calculated to be 3.92 eV and that of MoO$_3$ nanobelts and nanowires is estimated to be 3.06 eV.

REFERENCES

1. J.J. Auborn and Y.L. Barberio, *J. Electrochem. Soc.*, **134**, 638 (1987).
2. A. Katrib, D. Mey and G. Maire, *Catal. Today*, **65**, 179 (2001).
3. E. Comini, L. Yubao, Y. Brando and G. Sberveglieri, *Chem. Phys. Lett.*, **407**, 368 (2005).
4. J.N. Yao, K. Hashimoto and A. Fujishima, *Nature*, **355**, 624 (1992).
5. H.X. Zhang, Y.F. Li, Z.S. Hong and M.D. Wei, *Mater. Lett.*, **79**, 148 (2012).
6. Z.Y. Wang, S. Madhavi and X.W. Lou, *J. Phys. Chem. C*, **116**, 12508 (2012).
7. J. Rajeswari, P.S. Kishore, B. Viswanathan and T.K. Varadarajan, *Electrochem. Commun.*, **11**, 572 (2009).
8. J. Zhou, N.S. Xu, S.Z. Deng, J. Chen and J.C. She, *Chem. Phys. Lett.*, **382**, 443 (2003).
9. W. Merchan-Merchan, A.V. Saveliev and A.M. Taylor, *Micron*, **40**, 821 (2009).
10. Y.Z. Lei, J.C. Hu, H.W. Liu and J.L. Li, *Mater. Lett.*, **68**, 82 (2012).
11. X.W. Lou and H.C. Zeng, *Chem. Mater.*, **14**, 4781 (2002).
12. C.V. Krishnan, J. Chen, C. Burger and B. Chu, *J. Phys. Chem. B*, **110**, 20182 (2006).
13. Z.Q. Wang, H.F. Wang, C. Yang and J.H. Wu, *Mater. Lett.*, **64**, 2170 (2010).
14. L.L. Cai, P.M. Rao and X.L. Zheng, *Nano Lett.*, **11**, 872 (2011).